021884

NASA Technical Memorandum 110283

Finite Difference Radiative Transfer Model Calculations Compared to Measurements at the Top and Bottom of the Atmosphere

Stuart R. LeCroy
Analytical Services and Materials, Hampton, Virginia

Charles H. Whitlock
Langley Research Center, Hampton, Virginia

John T. Suttles
Hughes STX Corporation, Greenbelt, Maryland

January 1997

National Aeronautics and
Space Administration
Langley Research Center
Hampton, Virginia 23681-0001

TABLE OF CONTENTS

Summary

A finite difference radiative transfer program was developed to handle most anisotropic scattering and reflectance problems encountered in the Earth's atmospheric system. The model has been used to reproduce the radiance received by both satellite and ground based radiation measuring instruments. It accurately replicates the radiance measured by both narrow and wide field-of-view instruments with either narrow or broadband wavelength ranges located on the surface and at satellite altitudes. The output of the finite difference code is compared to the measurements by surface pyranometers and a spectroradiometer aboard a high flying aircraft. The program output is also compared to ERBE measurements aboard the ERBS and NOAA-9 satellites as well as the visible bands aboard the GOES-6 and GOES-7 satellites and AVHRR bands 1 and 2 of the NOAA-9 and NOAA-11 satellites. The model is within 0.2 % of the radiance received by pyranometers, within 0.6 % of the ERBE radiances, and within 3 % of the radiances measured by the visible bands of the GOES and NOAA AVHRR radiometers.

Introduction

A broad range of numerical techniques has been developed to describe the transfer of the solar radiation throughout the Earth's atmosphere system. Many methods do not have the necessary enhancements to include all orders of anisotropic scattering and surface bidirectional properties. Computer modeling of complex theoretical problems has improved to the point that accurate and fast calculations of atmospheric radiative transfer is now possible. Detailed maps of the spectral and angular radiation fields at the top and bottom of the atmosphere can now be generated. These radiance fields can be used to calibrate surface and satellite instruments, design new sensors, or study instrument performance characteristics.

In order to study radiation properties of the atmosphere in a realistic manner, radiative transfer models must include spectral, zenith, and azimuthal variations throughout the atmosphere. They should be able to handle any combination of angles and geometry involving the sun, a surface target point, and a satellite viewing platform. The transfer model should have the flexibility to change the range and step size of the program variables that include the angles that describe the hemispherical radiance field, phase function, altitude structure, and spectral variations. The surface bidirectional model should handle highly anisotropic spectral variations that account for zenith and azimuthal changes as well as moisture effects. Realistic up-to-date atmospheric and optical properties should be easily input. It is also very important to establish a range of validation checks on the program output. These validations are accomplished by making comparisons with other similar programs and, more importantly, by comparing the program output to measurements from instruments located on the surface and aboard satellites.

A radiation code has been developed that will handle the above requirements. It is able to simulate most anisotropic scattering and reflectance problems encountered in the Earth's atmospheric system. The program is flexible in changing of system state variables and is sufficiently sophisticated to handle surface and atmospheric physical and optical characteristics. This report describes the transfer model and some of its many applications. Measured atmospheric properties and surface reflectance data are input to the model, and radiance values are calculated for both the top-of-the-atmosphere (TOA) and the surface. Calculated results are then compared with measurements from both surface-based and satellite radiometers.

In order to compare the output of a radiation transfer program to radiometers, model inputs must represent the surrounding conditions under which the instruments operate. Atmospheric and optical properties must be obtained at the same operating time and at the radiometers location. Also, the input surface features should be representative of the scene viewed by the radiometers at any solar or viewing angle.

Modeling approach

The radiation transfer code used in this report is the Finite Difference Model (FD) developed by Barkstrom (1976) and Suttles (1981). The model includes multiple scattering, full zenith and azimuth angle variations, detailed spectral variations, and reflections by an anisotropic surface. The model fully describes both the incoming and the reflected hemispherical radiation fields at the bottom of the atmosphere and the outgoing field at the top of the atmosphere. The FD code uses the integro-differential equation given by Chandrasekhar (1960) for the case of a plane-parallel atmosphere. In order to digitize the computational process, the radiance field is expanded in a Fourier cosine series in azimuth and the phase function is expanded in a series of Legendre polynomials. Rather than using optical depth as the independent variable, the FD method expresses the equation of transfer in terms of altitude. The FD code is based on discretizing the depth and angular coordinates and approximating the integrals in Chandrasekhar's equation by Guassian quadrature formulas.

The FD model includes scattering by molecules and aerosols, and absorption by ozone, oxygen, water vapor, and aerosols. The scattering and absorption coefficients used in the FD model are a product of the atmospheric constituents cross sections and its vertical number densities. Atmospheric vertical properties are obtained from balloon-borne radiosondes and supplemented by local weather service soundings. The molecular scattering is described by the standard Rayleigh cross section coefficient proportional to the inverse fourth power of wavelength and a 2-term phase function. The total vertical number density is derived from current and local atmospheric soundings. Absorption cross sections for oxygen are derived from the values given in Bird and Riordan (1985). These coefficients are a combination of absorption coefficient and absorber amount since oxygen has a nearly constant distribution throughout the atmosphere.

Exponential-sum fitting methods have been used for water vapor absorption cross section for wavelengths of 0.94 microns and above with the equivalent coefficients taken from Stephens (1978). In order to account for the many types of spectral variations associated with satellite and ground based radiometers in the visible and near-infrared regions, additional water vapor cross section coefficients for wavelengths less than 1 micron have been derived from Bird and Riordan (1985). The Bird and Riordan coefficients have been normalized to the exponential-sum fitting method at the 0.94 micron wavelength. The water vapor density vertical profile is derived from current and local atmospheric soundings.

Aerosol characteristics are determined by inversion of the columnar aerosol optical depth (King et al. 1978) to obtain the size distribution. The optical depths are determined from solar photometers fitted with several filters in the visible and near-infrared spectral range. The aerosol size distribution is then inserted into a Mie code to determined the cross section scattering and absorption coefficients and the phase function. An Elterman shape (McClatchey et al. 1972) is assumed for the vertical number density of aerosols. This aerosol vertical distribution is further scaled by the columnar optical depth obtained from the solar photometers.

Ozone cross section coefficients for the ultraviolet and visible wavelengths are obtained from the tabulated values of Ackerman (1971). The vertical ozone number densities were obtained from McClatchey et al. (1972) and supplemented with values derived from orbiting SBUV (Solar Backscattering Ultraviolet) instruments. The vertical distribution is further scaled by the columnar ozone optical depth, which is derived from solar photometers by using the method of King and Bryne (1976).

The boundary conditions for the FD program include a variety of input conditions at the top and bottom of the atmosphere. These conditions are necessary to carry out studies relating to surface types, viewing conditions, and solar positions expected in the study of atmospheric radiation problems. The spectral solar irradiance incident at the (TOA) was taken from values given in Neckal and Labs (1984). These values have been further corrected for time-of-year effects.

Surface reflection properties include both diffuse and specular bidirectional effects. Satellite and ground studies have shown that most surfaces are non-Lambertian and highly anisotropic. In order to account for any possible surface effect, the FD surface bidirectional model has been devised to include influences from viewing elevation and azimuth, solar elevation, spectral variations, and soil moisture content. To be used by the program, experimentally-measured bidirectional data must be input in terms of Fourier cosine coefficients. For these studies, spectral bidirectional data were obtained by helicopter measurements as described in Whitlock et al. (1987) and Whitlock et al. (1994b).

The FD model is in good agreement with other radiation transfer codes. It was compared to other models under the Intercomparison of Radiation Codes in Climate Models (ICRCCM) format (Ellingson and Fouquart, 1990) and in a report on radiative transfer methods (Lenoble, 1985). In addition, the model was used in the comparison of aircraft results and in the calibration of satellite radiometers (Whitlock et al. 1985, Whitlock et al. 1990, and Whitlock et al. 1994a).

Experimental Verification

Because the FD program gives the entire hemispherical radiance field, it is an ideal tool to study and simulate the various radiation measuring instruments with different field-of-views used at the top and bottom of the atmosphere. By identifying the appropriate viewing angles in the hemispherical field, the model yields the radiation sensed by a narrow beam radiometer on board a satellite or a solar photometer located on the surface of the earth. By integrating over the hemispherical field, the FD program replicates the radiance sensed by a wide field-of-view pyranometer. Of course, the results from the simulation must be convoluted with the spectral response of the instruments and integrated over the instrument's active spectral range.

Comparison with broadband surface pyranometers

FD simulations were compared with bottom-of-atmosphere measurements from a Eppley PSP pyranometer taken during experiments conducted in the Sonora Desert in

Eppley PSP pyranometer taken during experiments conducted in the Sonora Desert in 1985. The results, shown in Fig. 1, are a good demonstration of the model's absorption and scattering properties. To obtain the radiance values to compare with the pyranometer, the program's output was integrated over the half sphere and the pyranometer's spectral range. Differences in the magnitudes are caused by sampling the pyranometer at different times during the day coinciding with overpass times of the NOAA-9 and ERBS satellites. Small perturbations in the pyranometer's output were noticed at some of the sampling times. These perturbations were assumed to be interferences from cirrus clouds. No attempt was made to simulate cirrus clouds to isolate these small fluctuations. The FD results without cirrus clouds average 0.2 % higher than the Eppley values, while the FD results including the cirrus clouds average 0.8 % lower than the Eppley values. Calibration uncertainty in the Eppley pyranometer values is estimated at 1.5 %.

Comparison with aircraft spectroradiometer

To ascertain the accuracy of the surface model in the FD program, the output of the program at the TOA was compared to the output of the spectroradiometer aboard a NASA U-2 aircraft (G. R. Smith, personal communication, 1985). At an altitude of 19 km, the U-2 is above 95 % of the Earth's atmosphere and only the attenuation effects of stratospheric ozone and aerosols at higher altitudes than the U-2 are not accounted for in the aircraft data. For this time period, the stratospheric aerosols are nearly at their background values, and as a result, have little effect on signal attenuation. Correcting the U-2 data for absorption by the Chappuis ozone band as carried out by Abel et al. (1993) results in radiance values at the TOA. This comparison between the U-2 values and the FD model (Fig. 2) is also a good indication of the accuracy of the absorption coefficients of the program. The FD program is in good agreement with the output of the U-2 radiometer. The target was a site in the Mohawk Valley near Yuma, Arizona where bidirectional surface properties used in the program were obtained (Whitlock et al. 1987). Estimated uncertainty in the aircraft values is 3.5 % (Smith et al. 1988).

Comparison with ERBE

The ERBE (Earth Radiation Budget Experiment) instruments aboard the NOAA-9 and ERBS (Earth Radiation Budget Satellite) orbital platforms are ideal radiometers with which to compare the TOA output of the FD program. The ERBE scanner instruments were well calibrated (Lee et al. 1993) and the satellites made regular daylight overpasses over the Sonora Desert region where the surface bidirectional and atmospheric properties are well known (Whitlock et al. 1987). The Sonora Desert (Fig. 3) is a sparsely vegetated region consisting mostly of widely separated creosote bushes covering crusted, sandy soil. The Sonoran area is flanked by the marshy Colorado River basin to the west, black lava beds to the east, mountains to the north and northeast, and the Gulf of California to the south.

Associated with the ERBE line-scanning radiometer system is their spatial response or point spread function (PSF) (Whitlock et al. 1989), so that results from the FD program have to include the effects of the PSF. The 99 % effective field-of-view at the satellite for the PSF is 5.16 degrees along the satellite heading and 9.13 degrees across the satellite heading. The ground coverage for 92 % of the PSF signal for both the ERBS and NOAA-9 satellite instruments is shown in Figs. 4 and 5, respectively. Since the satellites have different orbital paths and altitudes, their PSF ground coverages are somewhat different. The ERBS satellite was in a 57 degree inclination, 610 km altitude orbit, and passed over the Sonora Desert from north to south in the daylight hours. The NOAA-9 satellite had an orbital inclination of 99 degrees, an orbital altitude of 850 km, and passed over the Sonora Desert from south to north during the daylight hours. As seen in the PSF ground coverage figures, the ERBE values selected to compare with the FD output have to be carefully chosen to keep from being contaminated by the surrounding mountains, rivers, lava beds, or Gulf. The 100 % response range from both instruments of the two satellites will always contain some influence from the surrounding formations, more so for the NOAA-9 instrument because of its larger ground footprint due to the higher altitude orbit..

During the time that the bidirectional and atmospheric properties of the Sonora Desert were obtained, 11 sites were selected for the ERBS ERBE instrument and 3 sites were selected for the NOAA-9 ERBE instrument (Fig. 6) to use in the comparison with the FD output. These sites were selected based on the ERBS and NOAA-9 daytime overpass history and their location within the Sonora Desert. The TOA radiance data for the ERBS and NOAA-9 system were then obtained from the ERBE archive. Using the surface bidirectional data given in Whitlock et al. (1987) and atmospheric and optical properties obtained at the same time at a site along the U. S.-Mexico border, simulations to obtain TOA radiance values for the 14 chosen sites were carried out. Because the sites of the selected ERBE ground points are not the same as the U. S.-Mexico border site, a correction for ground reflectivity was made. NOAA-9 band 1 AVHRR data were used to correct for the differences in reflectivity by multiplying the FD output by the ratio of the value of the AVHRR pixel at the ERBE sites divided by the value of the AVHRR pixel at the border site. The maximum difference in satellite overpass time between the ERBS and NOAA-9 satellite was 2 hours. To correct the FD output for the effects of the PSF, the AVHRR band 1 scene was convoluted with the PSF so that each of the resulting individual pixels looks like those from an ERBE instrument. Multiplying the output of the FD program by the ratio of the value of the convoluted AVHRR pixel at the ERBE sites divided by the value of the unconvoluted AVHRR pixel at the ERBE sites should properly correct for PSF effects. Table 1 shows the results of these corrections on the FD output as computed radiances along with radiances obtained from the ERBE instruments. Also listed are the date the data were obtained and the site points as depicted in Fig. 6. An examination of the pyranometer traces reveals small variations at the time some of the data were obtained. These variations were attributed to cirrus clouds, however, no attempt was made to verify this by simulations. The results in Table 1 are also displayed in Fig. 7. This figure and Table 1 reveal that the FD results without cirrus clouds average 0.6 % higher than the ERBE values, while the FD results including cirrus clouds average 1.2 % higher. These results are encouraging considering that the atmospheric and surface measurements used as input to the FD model have at least a 5 % uncertainty.

Comparison with other TOA values

Another check on the accuracy of the FD radiative transfer code is to compare its TOA values to the output of other systems that calibrate satellite radiometric sensors. Other researchers use different combinations of surface measurements and radiative transmission equations to arrive at TOA radiance values, but NASA Goddard Space Flight Center utilizes a spectroradiometer on a high flying ER-2 aircraft which requires only minor output corrections to determine TOA values (Abel et al. 1993). This well-calibrated Goddard system will provide a good reference source to compare the TOA output of the FD program because it does not require any ground measurements or approximating equations. Flying at an altitude of 19 km, the ER-2 is above 95 % of the Earth's atmosphere. Normally only a small correction (less than 3 % of the total signal) is needed because of the absorption by the Chappius band of stratospheric ozone. The effects of stratospheric aerosols are usually small unless there has been a recent major volcanic eruption. The spectroradiometer aboard the ER-2 is calibrated before and after each flight. To obtain TOA measurements that are compatible with satellite sensors, the ER-2 is flown on a parallel track between the satellite and the surface target. The ER-2 is flown at the same time of the satellite overpass and its spectroradiometer maintains the same target viewing geometry as the satellite sensor.

Calibrating ER-2 flights are normally carried out over the sand dunes at White Sands Missile Range (WSMR), NM (Fig. 8). The Automated Radiometric Data Acquisition System (ARDAS) operated by Langley Research Center was located on the nearby alkali flats region. Its purpose was to accumulate a clear-sky surface climatological history in which parameters such as optical depths, albedos, incoming and reflected radiation could be found (Wheeler et al. 1994). These parameters, along with surface bidirectional data determined for the flats region (Whitlock et al. 1994b), provide sufficient input to the FD program to compute TOA radiance values to compare with satellite sensors recently calibrated by the ER-2 technique.

ER-2 overflights of the WSMR have been used to calibrated satellite radiometers aboard GOES-6, GOES-7, NOAA-9, and NOAA-11 (Abel et al. 1993, Abel et al. 1992, and Rao, 1993) during the time of the ARDAS operation. The uncertainty in the calibration values obtained using the ER-2 system is 4.3 %. The date and time for 11 separate comparison opportunities were identified during the period of operation of the ARDAS site and the appropriate FD computer runs were made to obtain TOA radiance values. The ER-2 calibrated satellite radiance values along with the FD output are shown in Table 2. Only the visible band from the GOES satellite is used. As listed in the table, there could be up to 2 days difference between the ER-2 calibration time and the simulation time. Only the nearest clear-sky day as determined by pyranometers was used. For easier comparison, the ER-2 data are plotted against the FD model results for band 1 in Fig. 9 and band 2 in Fig. 10. The FD results for band 1 average 4.6 % higher than the ER-2 calibrated GOES and AVHRR values. However, the GOES-6 data seem too low; and without this point, the FD results are only 3.0 % higher than the ER-2 values. The band 2 FD results (Fig. 10) average 6.4 % higher than the ER-2 calibrated AVHRR values. Surface moisture and atmospheric water vapor have a greater effect on AVHRR band 2 than band 1. The water vapor vertical structure used in the FD program was inferred from surface readings at the ARDAS site and readings from the top of the Sacramento Mountains, some 60 km from the ARDAS site. This separation distance could introduce some errors in determining the upper atmosphere water vapor profile over the ARDAS site. In addition, for two of the dates there were up to 2 days difference in simulation and ER-2 flight times. These spatial and temporal differences are the most likely cause of the higher FD values for band 2.

Conclusions

The FD atmospheric radiative transfer code is a valuable tool for analyzing both satellite and ground based radiation measuring instruments. The FD code has been able to accurately replicate the radiance received by a variety of radiometers (narrow and wide fields of view; narrow and broad spectral bands) both on the surface of the Earth and at the TOA. By duplicating the hemispherical radiance field at the top and bottom of the atmosphere, the radiance received by a radiometer at any zenith or program needs a complete surface reflectance model and realistic atmospheric physical and optical properties. For clear-sky days the output from the FD code approximates the radiance received by a pyranometer within about 0.2%. The code faithfully reproduced the radiances received by spectroradiometer on a high flying aircraft in the visible and near-infrared wavelengths. Also for clear-sky days, the radiance received by the ERBE radiometers aboard the ERBS and NOAA-9 satellite was approximated within about 0.6 %, and the visible bands of the GOES and NOAA AVHRR radiometers within about 3 %. A difference of about 6.4 % when compared to the AVHRR near-infrared band 2 is probably due to an error in determining the vertical structure of water vapor at the ARDAS site. The use of realistic atmospheric and optical properties along with anisotropic surface features is essential in simulating the radiance sensed by satellite radiometers.

Acknowledgements

The authors are indebted to Dr. Robert A. Schiffer (World Climate Research Programme Radiation Projects Office, NASA Headquarters), Dr. James C. Dodge (NASA Headquarters), and Dr. Bruce R. Barkstrom (ERBE Project Scientist) for their guidance and support during these experiments.

References

Abel, P. B., R. N. Galimore, and J. W. Cooper, 1992: Radiometric gains of satellite sensors of reflected solar radiation: Results from NASA ER-2 aircraft measurements. IGARSS Symposium, Houston, TX, 802-805.

------, B. Guenther, R. N. Galimore, and J. W. Cooper, 1993: Calibration results for NOAA-11 AVHRR channels 1 and 2 from congruent path aircraft observations. *J. Atmos. Oceanic Technol.*, **10,** 493-508.

Ackerman, M., 1971: Ultraviolet solar radiation related to mesospheric processes. G. Fiocco, Ed., D. Reidel Publishing Company, Dordrecht-Holland.

Barkstrom, B. R., 1976: A Finite Difference Method of solving anisotropic scattering problems. *J. Quant. Spectrosc. Transf.,* **16,** 725-739.

Bird, E. B., and C. Riordan, 1985: Simple solar spectral model for direct and diffuse irradiance on horizontal and tilted planes at the Earth's surface for cloudless atmospheres. *J. Climate Appl. Meteor.,* **25,** 87-97.

Chandrasekhar, S., 1960: *Radiative Transfer.* Dover Publications, 393 pp.

Ellingson, R. G., and Y. Fouquart, 1990: The intercomparison of radiation codes in climate models (ICRCCM). WMO/TD-No. 371, 46 pp. (Available from World Meteorological Organization, Geneva)

King, M. D., and D. M. Byrne, 1976: A method of inferring total ozone content from the spectral variation of total optical depth obtained with a solar radiometer. *J. Atmos.*

Sci., **33,** 2242-2251.

------, D. M. Byrne, B. M. Herman, and J. A. Reagan, 1978: Aerosol size distribution obtained by inversion of spectral optical depth measurements. *J. Atmos. Sci.*, **35**, 2153-2167.

Lee, R. B. III, B. R. Barkstrom, S. L. Carman, J. E. Cooper, M. A. Folkman, P. J. Jarecke, L. P. Kopia, and B. A. Wielicki, 1993: The Clouds and the Earth's Radiant Energy System (CERES) Experiment, Earth Observing System (EOS) instrument and calibrations. *SPIE Proc.,* **1939,** 61-71.

Lenoble, J. (ed),1985: Radiative transfer in scattering and absorbing atmospheres: Standard computational procedures. A. Deepak Publishing, Hampton, VA.

McClatchey, R. A., R. W. Fenn, J. E. A. Selby, F. E. Voltz, and J. S. Garing, 1972: Optical properties of the atmosphere (Third Edition). Report No. AGCRL-72-0497, Air Force Cambridge Research Laboratories.

Neckal, H., and D. Labs, 1984: The solar radiation between 3300 and 12500 . *Solar Physics,* **90,** 205-258.

Rao, C. R. N. ,1993: Degradation of visible and near-infrared very high resolution radiometer on the NOAA-9 spacecraft: Assessment and recommendation for corrections. NOAA Tech. Rep. NESDIS 70, 25 pp.

Smith, G. B., R. H. Levin, P. Abel, and H. Jacobowitz, 1988: Calibration of the solar channels of the NOAA-9 AVHRR using high altitude aircraft measurements. *J. Atmos. Oceanic Technol.*, **5,** 631-639.

Stephens, G. L., 1978: Radiation profiles in extended water clouds. *J. Atmos. Sci.*, **35,** Stephens, G. L., 1978: Radiation profiles in extended water clouds. *J. Atmos. Sci.*, **35,** 2111-2122.

Suttles, J. T., 1981: Anisotropy of solar radiation leaving the earth-atmosphere system. Ph. D. thesis, Old Dominion University. (Available from NTIS, NASA Accession No. N82-32242).

Wheeler, R. J., S. R. LeCroy, C. H. Whitlock, G. C. Purgold, and J. S. Swanson, 1994: Surface characteristics for the alkali flats and dunes regions at White Sands Missile Range, NM. *Remote Sens. of Envir.*, **48**, 181-190.

Whitlock, C. H., J. T. Suttles, S. R. LeCroy, D. I. Sebacher, and W. H. Fuller, 1986: Evaluation of standard radiation aerosol models for a coastal environment. *J. Geophys. Res.*, **91**, 14491-14500.

------,G.C. Purgold, and S. R. LeCroy, 1987: Surface bidirectional reflectance properties of two southwestern Arizona deserts for wavelengths between 0.4 and 2.2 micrometers. NASA TP 2643.

------,W. F. Staylor, J. T. Suttles, G. Smith, R. Levin, R. Frouin, C. Gautier, P. M. Teillet, P. N. Slater, Y. J. Kaufman, B. N. Holben, W. B. Rossow, C. Brest, and S. R. LeCroy, 1990: AVHRR and VISSR instrument calibration results for both cirrus and marine stratocumulus IFO periods. Fire Science Report 1988. NASA CP 3083, 141-145.

------,L. W. Hoffman, and R. F. Arduini, 1989: ERBE/NOAA-9 observations for the FIRE/SRB Wisconsin experiment region from October 14 through October 31, 1986. NASA TM 101627.

impact on ISCCP. Paper 8ATRAD FA 1.1, AMS Conference on Atmospheric Radiation, Nashville, TN.

------,S. R. LeCroy, and R. J. Wheeler, 1994b: Narrowband angular reflectance properties of the alkali flats at White Sands, New Mexico. *Remote Sens. of Envir.,* In Press.

TABLE 1. TOA radiances for ERBE satellites.

Satellite	Date	Aim Point Number	Cirrus Clouds	Satellite Radiances [a]	Computed Radiances [a]
ERBS	14 MAY 85	1	NO	63.2	63.2
ERBS	14 MAY 85	2	NO	61.7	63.2
ERBS	14 MAY 85	3	NO	62.6	64.5
ERBS	14 MAY 85	4	NO	64.3	65.8
ERBS	14 MAY 85	5	NO	63.3	64.1
ERBS	13 MAY 85	6	YES	51.1	53.5
ERBS	13 MAY 85	7	YES	52.3	55.1
ERBS	20 MAY 85	8	YES	64.5	66.9
ERBS	20 MAY 85	9	YES	64.6	68.1
ERBS	20 MAY 85	10	YES	67.5	68.3
ERBS	20 MAY 85	11	YES	65.8	64.5
NOAA-9	13 MAY 85	1	NO	62.5	60.2
NOAA-9	14 MAY 85	2	NO	61.5	60.8
NOAA-9	14 MAY 85	3	NO	59.9	61.4

[a] Units are W m^{-2}-sr^{-1}

TABLE 2. TOA radiances for GOES and NOAA satellites.

	ER−2			FD		
Satellite	Date	Band 1[a]	Band 2[a]	Date	Band 1[a]	Band 2[a]
GOES−6	7 NOV 88	106	–	7 NOV 88	142	–
GOES−7	7 NOV 88	165	–	7 NOV 88	156	–
GOES−7	7 JUL 89	191	–	6 JUL 89	210	–
GOES−7	26 JUL 90	156	–	28 JUL 90	157	–
GOES−7	14 OCT 90	148	–	14 OCT 90	166	–
GOES−7	25 OCT 90	166	–	25 OCT 90	184	–
NOAA−9	11 NOV 88	46	29	9 NOV 88	46	30
NOAA−11	18 NOV 88	106	73	18 NOV 88	122	83
NOAA−11	7 JUL 89	223	123	6 JUL 89	203	135
NOAA−11	19 MAR 90	178	113	19 MAR 90	187	124
NOAA−11	25 OCT 90	128	83	25 OCT 90	137	92

[a] Units are $W\,m^{-2}-sr^{-1}-\mu m^{-1}$

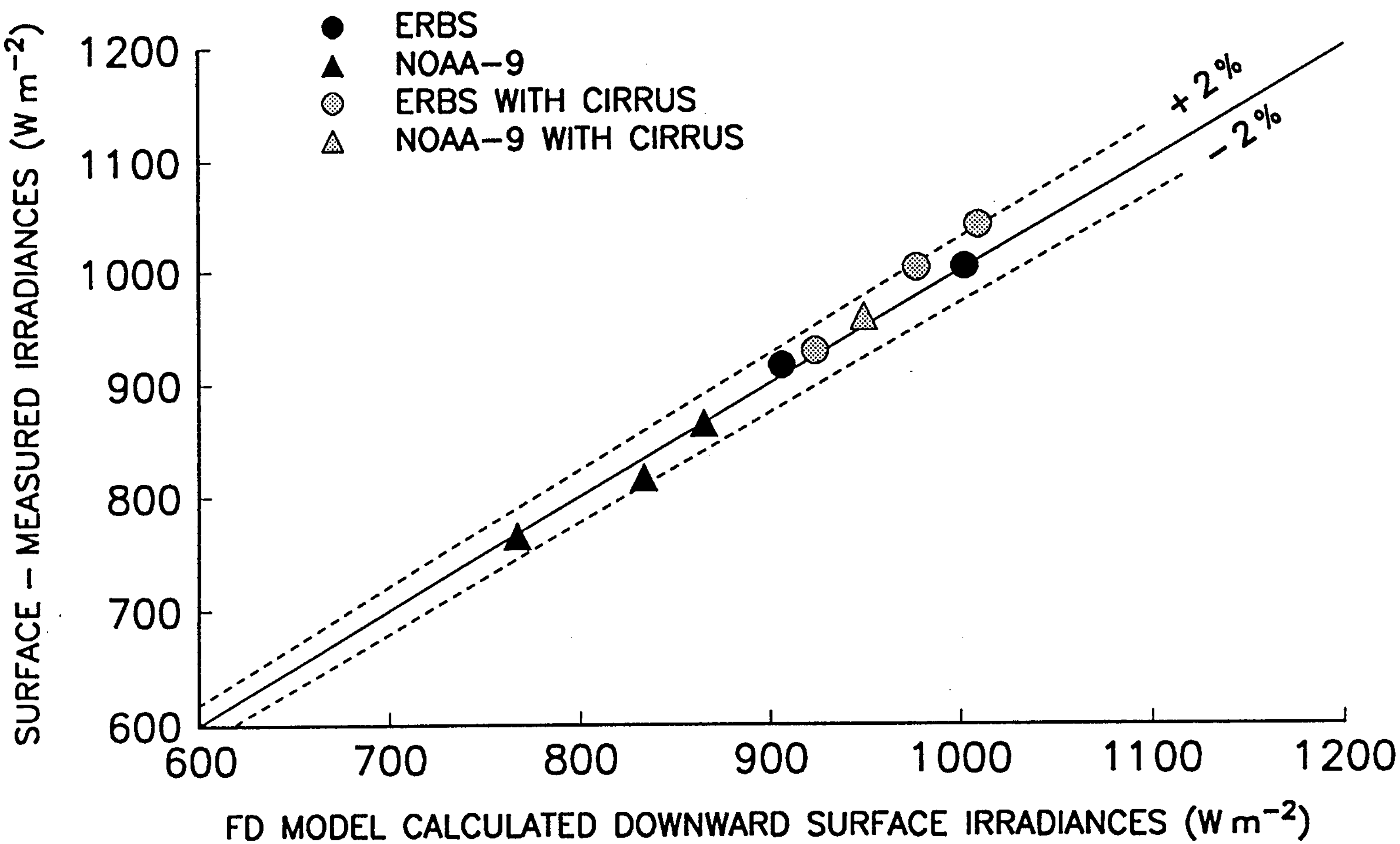

Fig. 1. Comparison of FD output with an Eppley pyranometer.

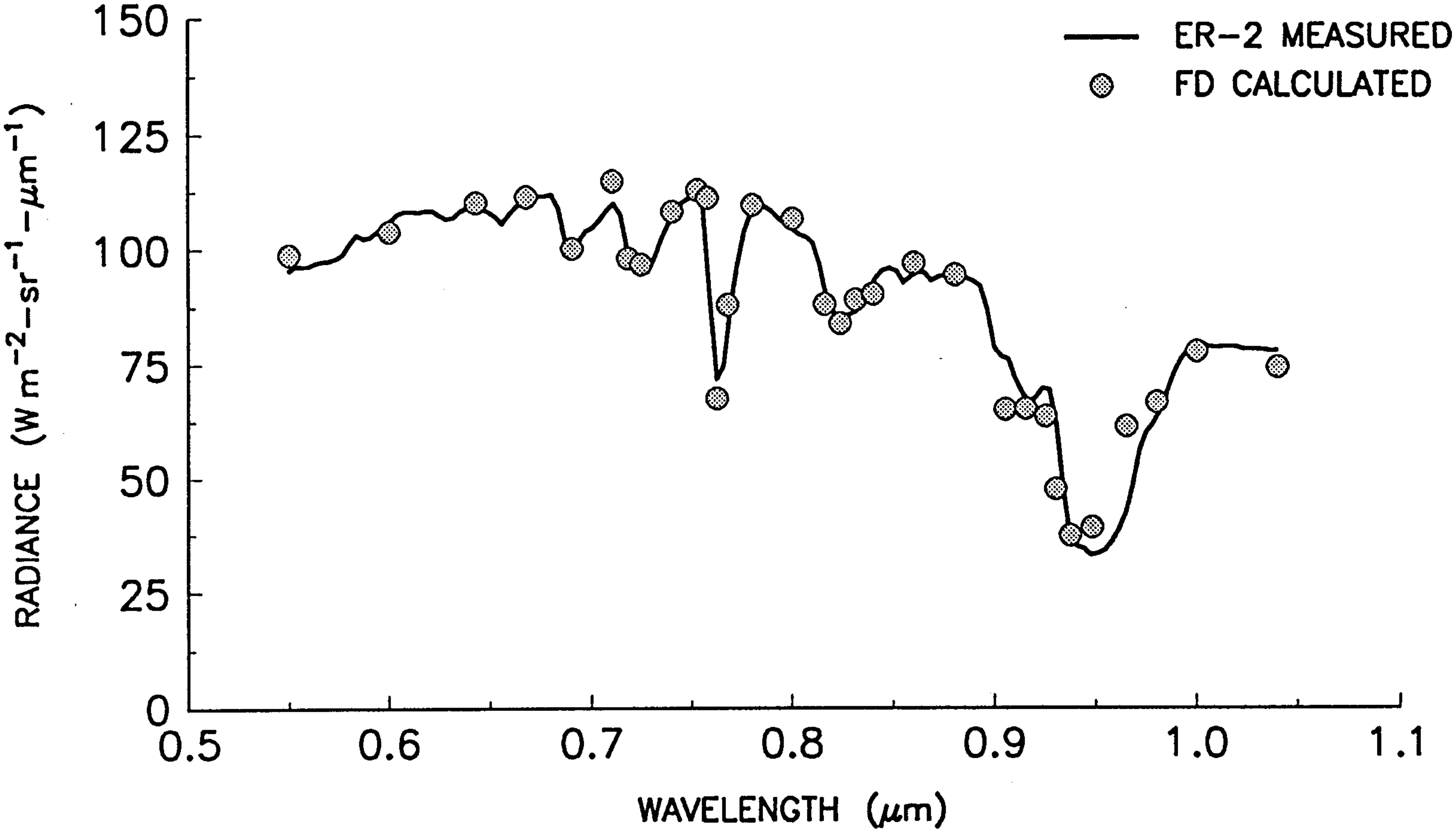

Fig. 2. Comparison of FD output with an ER−2 spectroradiometer.

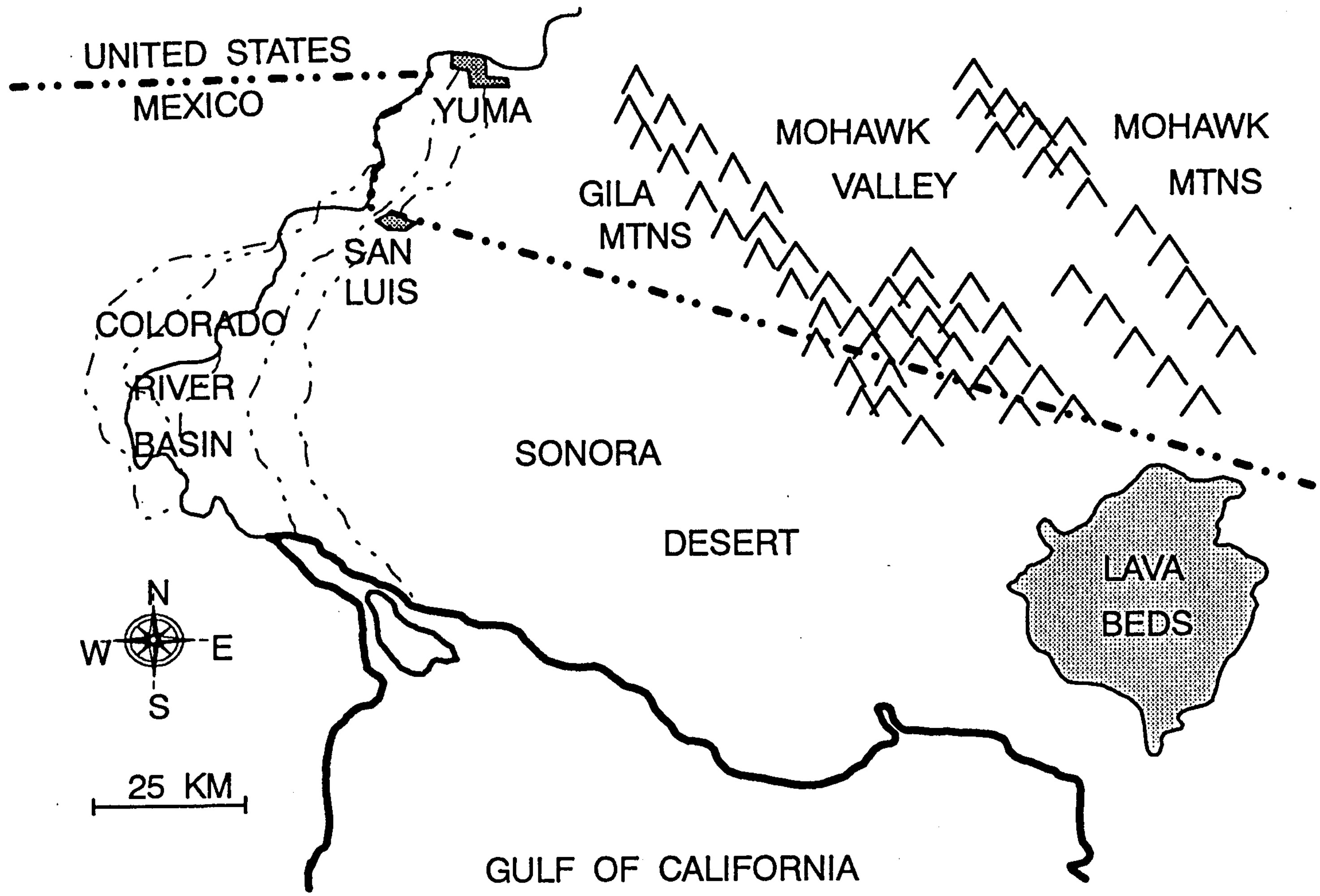

Fig. 3. Sonora Desert region.

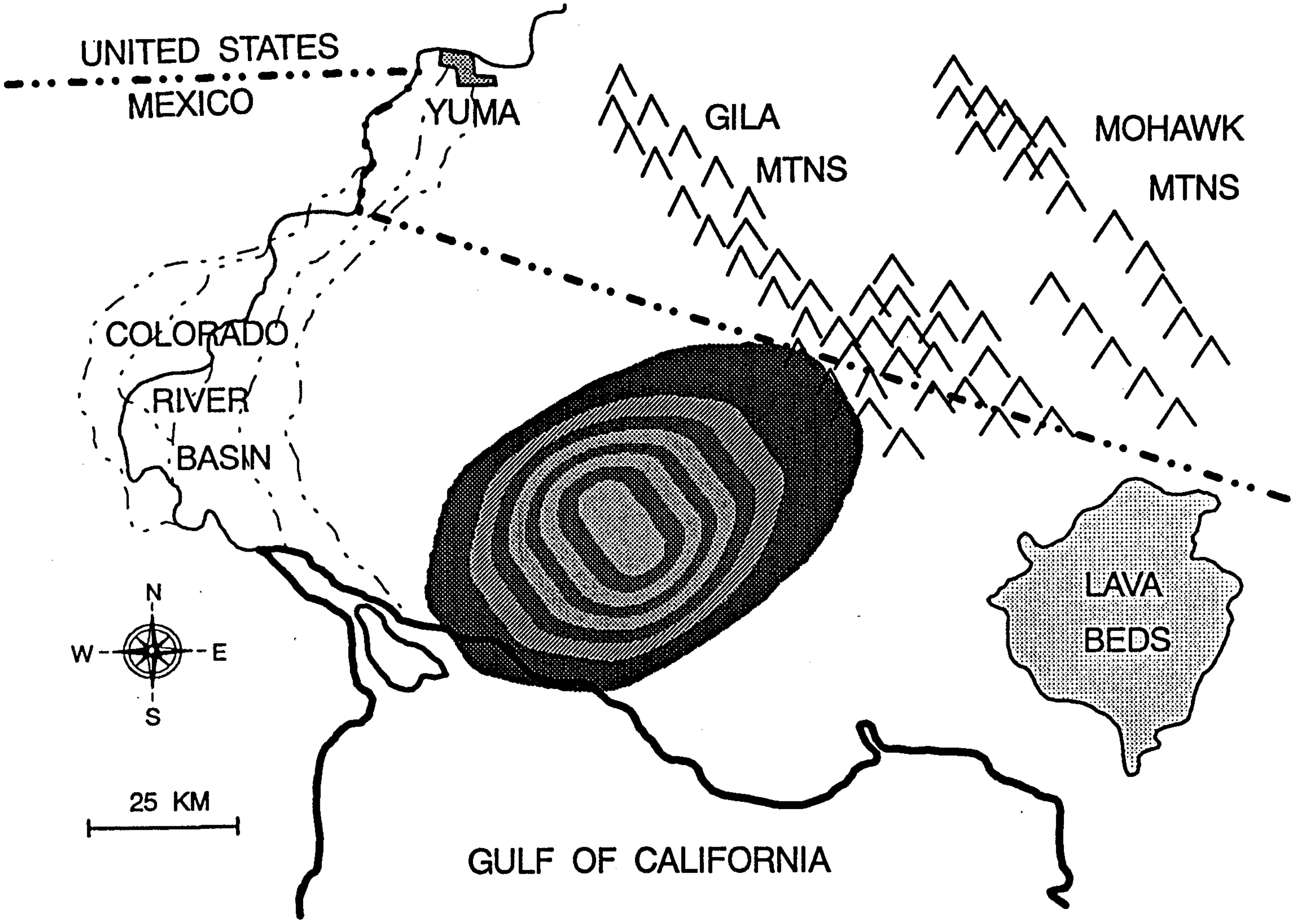

Fig. 4. Typical ground coverage contours of the PSF for ERBS. (Each band represents 11.5 percent of the received signal and the outer boundary equals 92 percent.)

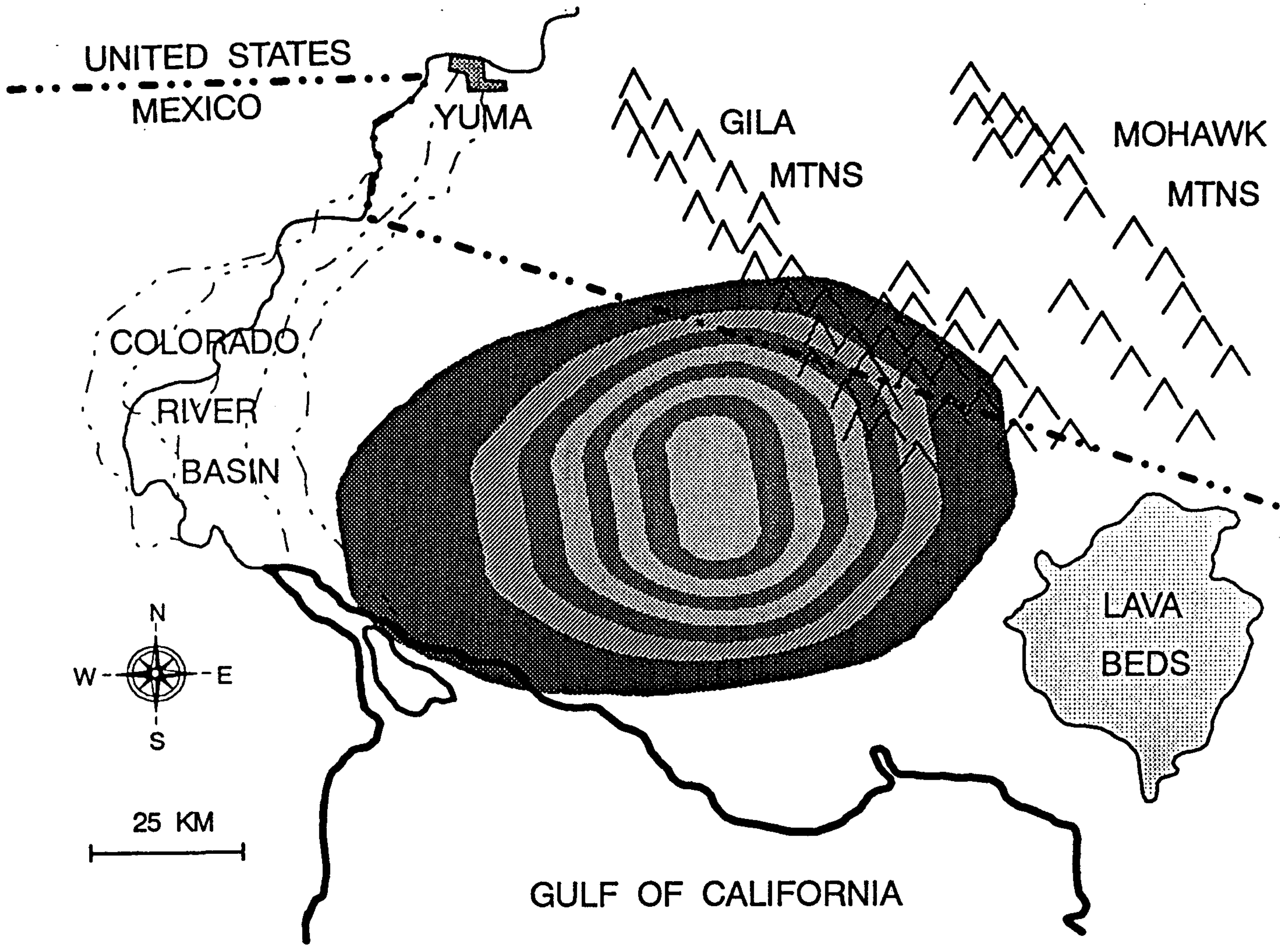

Fig. 5. Typical ground coverage contours of the PSF for NOAA-9. (Each band represents 11.5 percent of the received signal and the outer boundary equals 92 percent.)

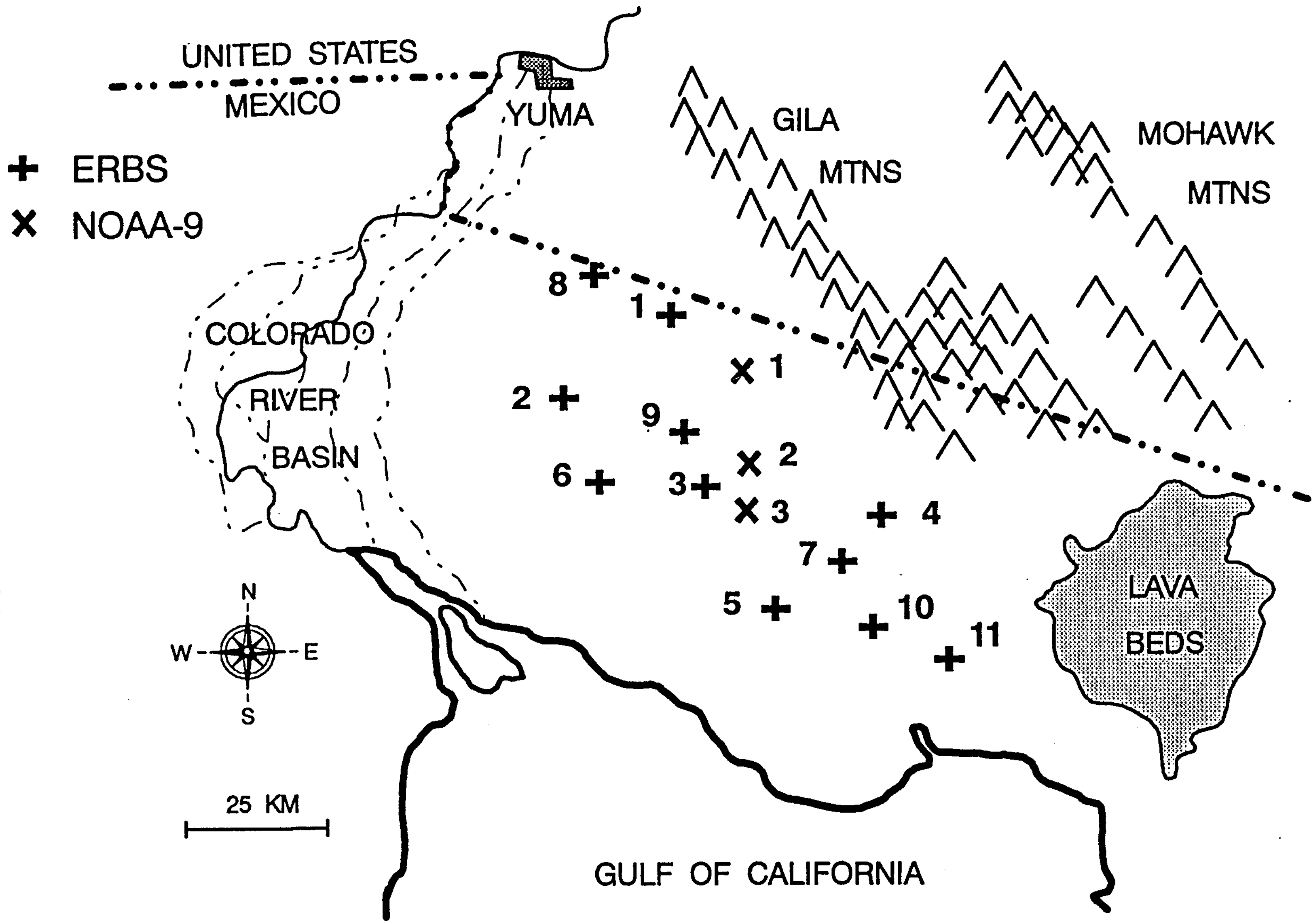

Fig 6. Location of ERBS and NOAA-9 aim points.

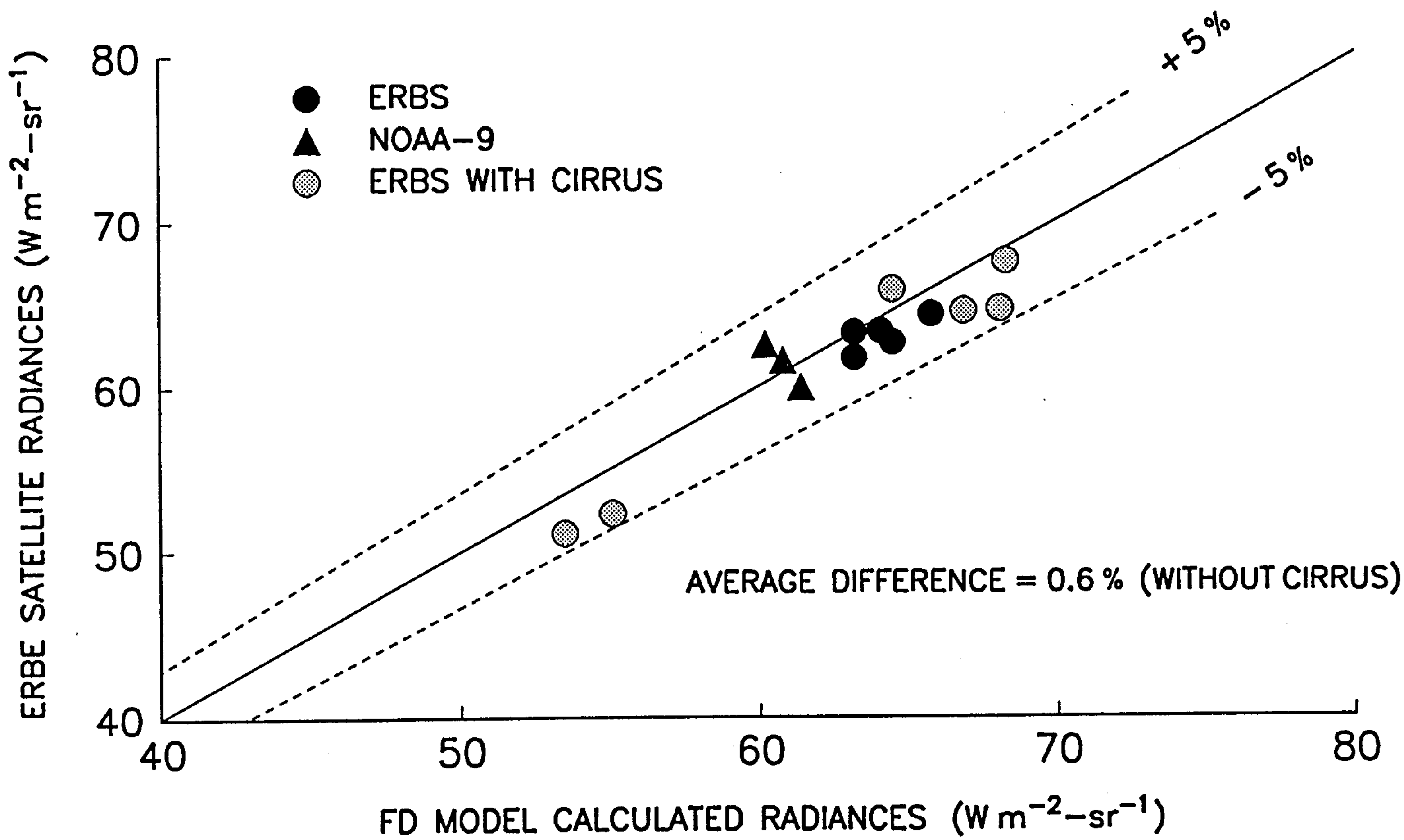

Fig. 7. Comparison of FD output with ERBE.

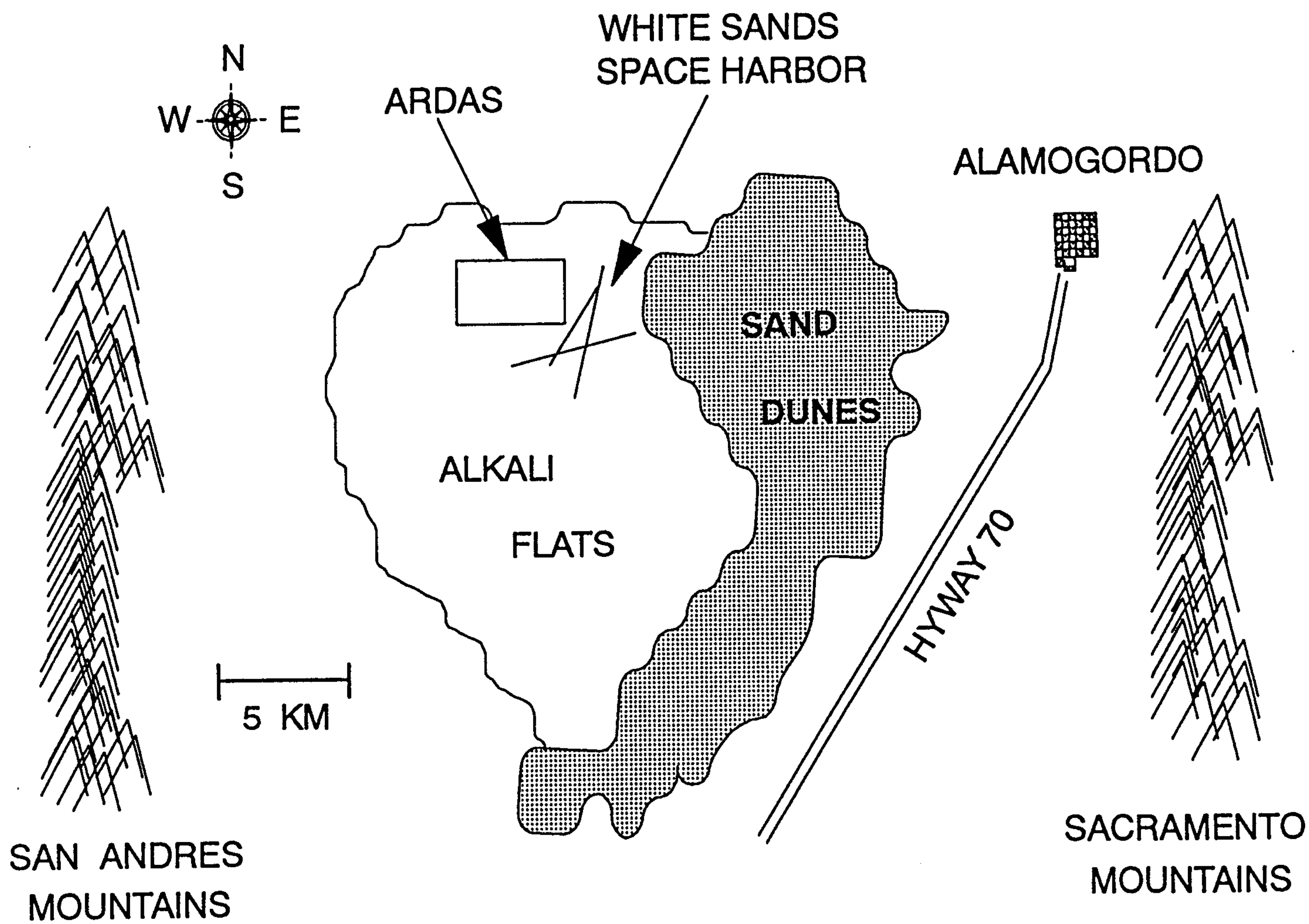

Fig. 8. White Sands Missile Range area.

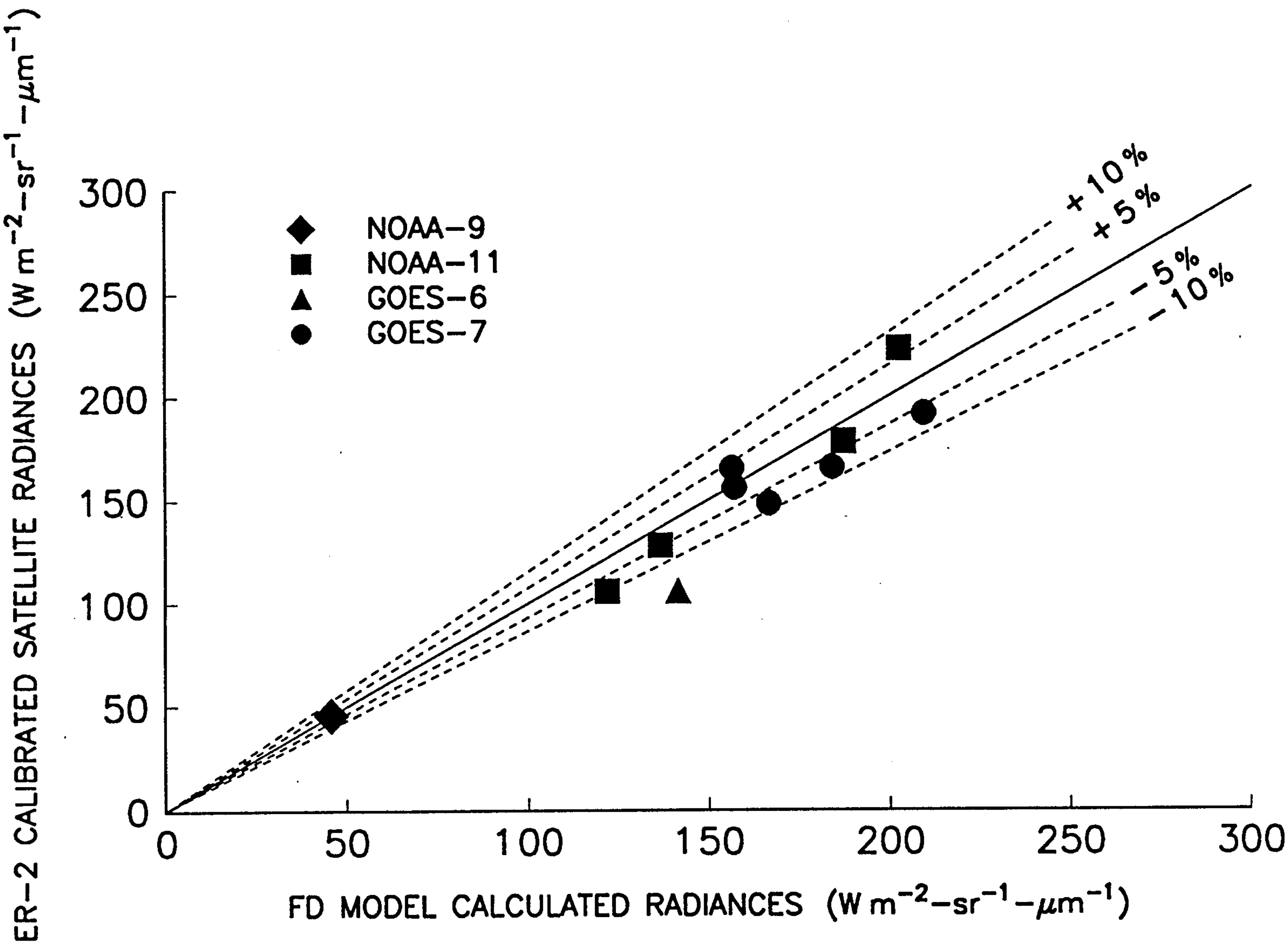

Fig. 9. Comparison of FD output with band 1 radiances.

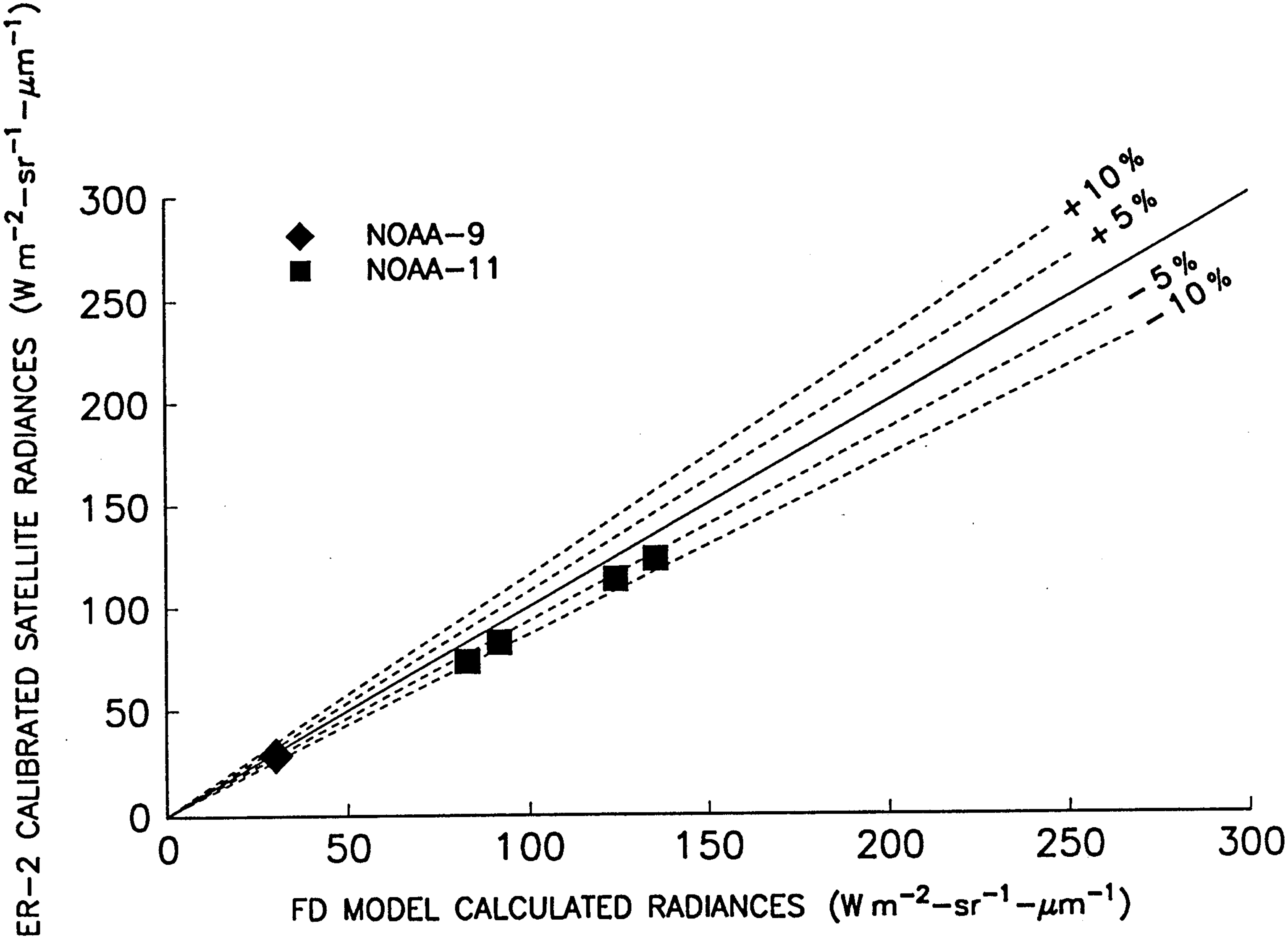

Fig. 10. Comparison of FD output with band 2 radiances.

REPORT DOCUMENTATION PAGE

Form Approved
OMB No. 0704-0188

1. AGENCY USE ONLY *(Leave blank)*	2. REPORT DATE	3. REPORT TYPE AND DATES COVERED
	January 1997	Technical Memorandum

4. TITLE AND SUBTITLE
Finite Difference Radiative Transfer Model Calculations Compared to Measurements at the Top and Bottom of the Atmosphere

5. FUNDING NUMBERS
148-65-41-01

6. AUTHOR(S)
Stuart R. LeCroy
Charles H. Whitlock
John T. Suttles

7. PERFORMING ORGANIZATION NAME(S) AND ADDRESS(ES)
NASA Langley Research Center
Hampton, VA 23681-0001

8. PERFORMING ORGANIZATION REPORT NUMBER

9. SPONSORING / MONITORING AGENCY NAME(S) AND ADDRESS(ES)
National Aeronautics and Space Administration
Washington, DC 20546-0001

10. SPONSORING / MONITORING AGENCY REPORT NUMBER
NASA TM-110283

11. SUPPLEMENTARY NOTES
LeCroy; Analytical Services and Materials, Hampton, VA; Whitlock; NASA Langley Research Center, Hampton, VA; Suttles; Hughes STX Corporation, Greenbelt, MD

12a. DISTRIBUTION / AVAILABILITY STATEMENT
Unclassified-Unlimited

Subject Category 47

12b. DISTRIBUTION CODE

13. ABSTRACT *(Maximum 200 words)*

A finite difference radiative transfer program was developed to handle most anisotropic scattering and reflectance problems encountered in the Earth's atmospheric system. The model has been used to reproduce the radiance received by both satellite and ground based radiation measuring instruments. It accurately replicates the radiance measured by both narrow and wide field-of-view instruments with either narrow or broadband wavelength ranges located on the surface and at satellite altitudes. The output of the finite difference code is compared to the measurements by surface pyranometers and a spectroradiometer aboard a high flying aircraft. The program output is also compared to ERBE measurements aboard the ERBS and NOAA-9 satellites as well as the visible bands aborad the GOES-6 and GOES-7 satellites and AVHRR bands 1 and 2 of the NOAA-9 and NOAA-11 satellites. The model is within 0.2% of the radiance received by pyranometers, within 0.6% of the ERBE radiances, and within 3% of the radiances measured by the visible bands of the GOES and NOAA AVHRR radiometers.

14. SUBJECT TERMS
Surface Radiation, ISCCP, ERBE, Clouds, Climate

15. NUMBER OF PAGES
33

16. PRICE CODE
A03

17. SECURITY CLASSIFICATION OF REPORT	18. SECURITY CLASSIFICATION OF THIS PAGE	19. SECURITY CLASSIFICATION OF ABSTRACT	20. LIMITATION OF ABSTRACT
UNCLASSIFIED	UNCLASSIFIED	UNCLASSIFIED	UL